

Voltammetric and Impedance Analysis of Dimethyldioctadecylammonium/Prussian Blue Langmuir–Blodgett Films on ITO Electrodes

Raphaël Saliba, Béatrice Agricole, Christophe Mingotaud, and Serge Ravaine*

Centre de Recherche Paul Pascal, CNRS, Avenue A. Schweitzer, F-33600 Pessac, France

Received: July 7, 1999

New hybrid Langmuir–Blodgett (LB) films containing Prussian Blue have been studied by cyclic voltammetry and electrochemical impedance spectroscopy. The dependencies of the cyclic voltammetry response on the number of deposited layers and the scan rate are described and show that the hybrid LB films can be considered as a quasi-reversible system with a finite diffusion space. On the basis of the impedance spectroscopy results, the charge transport process through the lamellar materials is modeled with an equivalent circuit considering two kinds of charge transport. The diffusion coefficients associated with the motions of the charged species are found to be very small, reflecting the fact that the insulating lipid layers considerably hinder the diffusion of the charged species.

Introduction

Since the initial report of the deposition of Prussian Blue (PB) in the form of a film on solid electrodes,¹ many studies of the electrochemical behavior of such films have been performed.^{2–16} It has been shown that electrodes modified with PB and related cyanometalate compounds exhibit many interesting properties that make them potentially applicable in areas such as electrochromism,^{17–19} catalysis,²⁰ photosensing devices,²¹ energy storage^{22,23} and ion-selecting sensors.³

Films of PB have been deposited on various substrates such as platinum, graphite, gold, SnO₂, and ITO, by simple immersion^{1–3} or by electrochemical methods.^{3,4,8,11} Even if actually there is no consensus on the best method to obtain high-quality deposits, the fact that the electrochemical response of the films is strongly dependent on their history and elaboration is uniformly adopted. It has been shown, for example, that soluble PB films (KFe[Fe(CN)₆]), which are obtained from the initially formed insoluble PB deposits (Fe₄[Fe(CN)₆]₃) by successive cycling around the reduction system PB/Everitt's salt (K₂Fe[Fe(CN)₆]) in KCl aqueous solutions, are more stable than their precursors against cycling around the oxidation system PB/Prussian Yellow (Fe[Fe(CN)₆]).^{14,16}

We recently reported the elaboration of a new type of PB modified electrodes, based on the build up of hybrid Langmuir–Blodgett films on ITO.²⁴ These new materials have a perfectly defined lamellar structure that can be described as a layer of cyanide-bridged irons intercalated between two layers of dimethyldioctadecylammonium (DODA) and present a ferromagnetic behavior below 5.7 K.²⁴ Preliminary investigations of their electrochemical properties in aqueous KCl solutions have exhibited a linear dependency of their voltammetric response, absorbance, and photoresponse on the number of deposited layers.²⁵ This interesting result suggests that the motion of charged species, i.e., electrons and potassium ions, through the LB films is easy.

In the past few years, cyclic voltammetry (CV) and impedance spectroscopy have been revealed as useful tools in the study of charge transport processes in conducting films,^{26–28} and in particular, in electrodeposited films of PB.^{29–31} Thus, cyclic voltam-

mograms and electrochemical impedance spectra of DODA/PB LB films on ITO electrodes have been carefully analyzed in order to obtain more detailed information about the transport of charged species during the redox reactions of these systems.

Experimental Section

Reagents and Materials. Prussian Blue, tetrabutylammonium bromide, and potassium chloride were purchased from Aldrich and dimethyldioctadecylammonium bromide (99%) was from Kodak. ITO glass slides were obtained from ICMC (France) and were cleaned by sequential sonication in acetone and distilled water prior to each experiment.

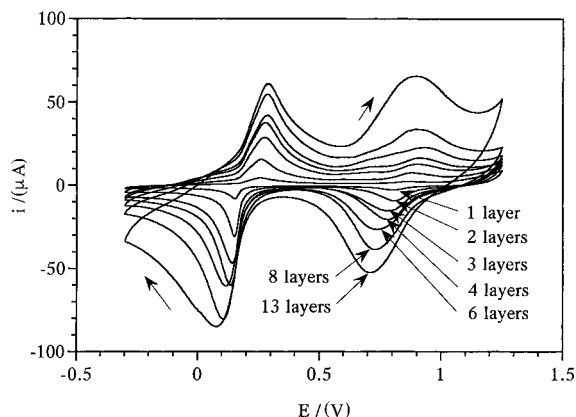
Procedures. Spreading solutions were prepared from HPLC grade chloroform (Prolabo) and were kept at –18 °C between experiments to limit solvent evaporation. An appropriate amount of the DODA solution was carefully spread onto a 10^{–5} M Prussian Blue aqueous solution so that the initial area per molecule was close to 200 Å², and the spreading solvent was allowed to evaporate for 10 min prior to compression. The Langmuir monolayers were compressed at 20 ± 1 °C using a step-by-step procedure. The Y-type DODA/PB LB films were obtained by the vertical lifting method with a transfer ratio close to unity, at a target pressure of 30 mN/m, with a dipping speed of 1 cm/min. After each cycle, the substrate was allowed to dry for 5 min in air.

Instrumentation. The LB experiments were carried out with a laboratory-made trough.³² The surface pressure was measured with a platinum Wilhelmy plate. A Millipore purification system produced water with a resistivity higher than 18 MΩ·cm for all experiments. All the electrochemical experiments were carried out in a three-electrode conventional cell, at the ambient laboratory temperature (20 ± 1 °C), in KCl aqueous solutions that had been bubbled with nitrogen for at least 20 min. The cyclic voltammetry and impedance spectroscopy experiments were conducted with an Autolab PGSTAT 20 potentiostat and a FRA module from EcoChemie, computer controlled by their General Purpose Electrochemical System and FRA softwares, respectively. Potentials were measured with respect to a saturated calomel electrode (SCE). Impedance measurements were carried out in the frequency range 10 kHz to 0.1 Hz with a signal amplitude of 10 mV. The stabilization potential was

* To whom correspondence should be addressed.

TABLE 1: Dependence of the Voltammetric Parameters on the Number of Transferred Layers of PB. Scan Rate: 0.05 V/s

no. of PB layers	E_p (V)	I_p ($\mu\text{A}/\text{cm}^2$)	Q_p ($\mu\text{C}/\text{cm}^2$)	$w_{1/2}$ (V)	E_{pa} (V)	I_{pa} ($\mu\text{A}/\text{cm}^2$)	Q_{pa} ($\mu\text{C}/\text{cm}^2$)	$w_{a1/2}$ (V)	E_{pp} (V)
1	0.151	9.4	27.3	0.061	0.254	4.8	33.6	0.122	0.103
2	0.150	28.4	53.9	0.060	0.261	13.3	53.3	0.132	0.111
3	0.142	43.1	113.0	0.095	0.273	23.8	92.2	0.144	0.131
4	0.134	55.4	158.4	0.103	0.276	30.4	110.1	0.146	0.142
6	0.117	64.4	189.9	0.139	0.286	33.2	144.6	0.151	0.169
8	0.106	71.7	275.7	0.159	0.284	44.1	196.1	0.161	0.178
13	0.083	76.5	444.9	0.242	0.286	52.2	321.5	0.183	0.203

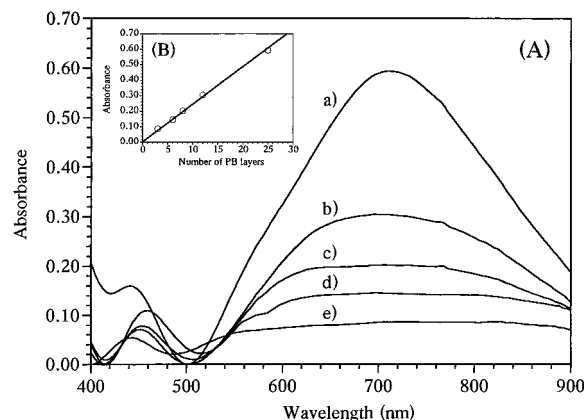
**Figure 1.** Cyclic voltammograms of DODA/PB LB films with 1, 2, 3, 4, 6, 8, and 13 layers of PB in aqueous 0.5 M KCl. Scan rate = 0.05 V/s. Area of the electrode $\approx 1 \text{ cm}^2$. Starting point of scanning: 0.5 V/SCE.

set to 0.2 V/SCE, which is the equilibrium potential of the DODA/PB LB films in a 0.5 M aqueous KCl solution. It has been shown that the impedance of electrodeposited PB films reaches a minimum value at this potential, which implies that a maximum value of the apparent diffusion coefficients could be expected.²⁹ The fitting of experimental data to an equivalent circuit was carried out by means of a complex nonlinear least-squares procedure (CNLS) (LEVIM 7.1 software³³). UV–visible spectra were recorded with an Unicam UV 4 spectrophotometer.

Results and Discussion

Cyclic Voltammetry. Cyclic voltammograms of DODA/PB LB films with 1, 2, 3, 4, 6, 8, and 13 layers of PB in 0.50 M KCl aqueous solutions are shown in Figure 1. As has been reported previously,²⁵ the voltammetric response of these hybrid materials is in agreement with the known electrochemical activity of PB films in aqueous potassium electrolytes, which consists of two sets of peaks corresponding to two reversible redox reactions of PB: its reduction to Everitt's salt and its oxidation to Prussian Yellow. Table 1 collects results of peak potential (E_p), peak-to-peak separation (E_{pp}), peak current (I_p), electrical charge (Q_p), and half-peak widths ($w_{1/2}$) corresponding to the anodic and cathodic peaks associated with the PB/Everitt's salt system. The increase in the areas of the peaks demonstrates that PB is homogeneously transferred during the elaboration of the LB films. This feature is in accord with the gradual increase of the absorbance of these materials shown in Figure 2A. It can be seen in Figure 2B that the intensity of the characteristic band of PB at 704 nm increases linearly with the number of PB layers.

The average increase in the area of the cathodic peak around 0.15 V/SCE on the CV curves (see Figure 1) after the transfer of one PB layer onto the ITO electrode corresponds to ca. $3.2 \times 10^{-10} \text{ mol} \cdot \text{cm}^{-2}$ of Fe^{III} . It is assumed that the redox reaction involves one electron change per each iron atom and that all PB is electroactive. Taking into account that the distance between two next-nearest Fe^{III} atoms in PB is 10.2 \AA ,^{34,35} this coverage corresponds to one single layer of $\text{Fe}^{\text{II}}\text{--Fe}^{\text{III}}$. This

**Figure 2.** (A) Absorbance spectra of DODA/PB LB films with (a) 25, (b) 12, (c) 8, (d) 6, and (e) 3 layers of PB. (B) Dependence of the absorbance at 704 nm on the number of PB layers.

result is in agreement with the previously reported structure of the DODA/PB LB films, which had been obtained by low-angle X-ray diffraction experiments.²⁴

Regarding the global shape of the voltammograms, one can note that the peak-to-peak separation and the half-peak widths increase with the number of deposited layers. Such behaviors can be partially explained if one considers the seducing model developed by Aoki et al.,^{36,37} which takes into consideration the diffusion of species through electroactive films thicker than one monolayer. According to this theory and assuming that each DODA/PB LB film behaves like a unique electroactive film, the experimental observations should be correlated to a decrease of the kinetics of the redox reaction and an increase of the thickness of the diffusion space. Such variations are consistent with the increasing number of insulating DODA layers, which probably hinder the diffusion of the charged species through the LB films. Nevertheless, the motion of these species is still effective even after the deposition of 13 layers of PB as a gradual increase of the peak current is shown in Figure 1. This result should indicate the presence of holes in the lipid films.

The electrochemical behavior of the DODA/PB lamellar systems has been further investigated by recording the CV curves at different scan rates, in the range 0.05–1 V/s. As example, the dependence of the voltammogram of a LB film containing three layers of PB on the sweep rate is shown in Figure 3. Results of peak potential, peak current, half-peak widths, and peak-to-peak separation corresponding to the peaks associated with the PB/Everitt's salt system are collected in Table 2. Both the half-peak widths and the peak-to-peak separation are found to increase with the scan rate, as a consequence of the ohmic drop effect due to the presence of five insulating DODA layers. The dependence of the peak current on the square root of the sweep rate is shown in Figure 4. A linear behavior is observed. Meanwhile, it has been observed that the variation of the potential of the peaks on the logarithm of the scan rate presents a concave shape (not shown). These results should indicate that the DODA/PB LB film could be considered as a quasi-reversible system with a finite diffusion

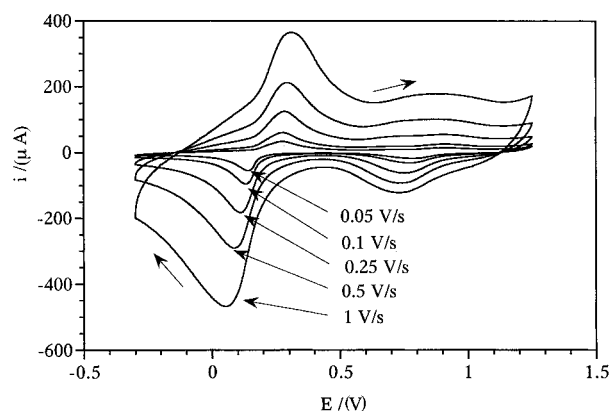


Figure 3. Dependence of the cyclic voltammogram of a DODA/PB LB film with 3 layers of PB on the scan rate. Supporting electrolyte: 0.5 M KCl. Area of the electrode $\approx 1 \text{ cm}^2$. Starting point of scanning: 0.5 V/SCE.

TABLE 2: Dependence of the Voltammetric Parameters on the Scan Rate for a LB Film with 3 Layers of PB

scan rate (V/s)	E_{pc} (V)	I_{pc} ($\mu\text{A}/\text{cm}^2$)	$w_{c1/2}$ (V)	E_{pa} (V)	I_{pa} ($\mu\text{A}/\text{cm}^2$)	$w_{a1/2}$ (V)	E_{pp} (V)
0.05	0.142	43.1	0.095	0.273	23.8	0.144	0.131
0.1	0.132	74.5	0.112	0.273	40.7	0.146	0.141
0.25	0.112	137.7	0.159	0.281	77.9	0.159	0.169
0.5	0.088	205.7	0.208	0.293	124.2	0.178	0.205
1	0.061	293.8	0.261	0.308	206.1	0.210	0.247

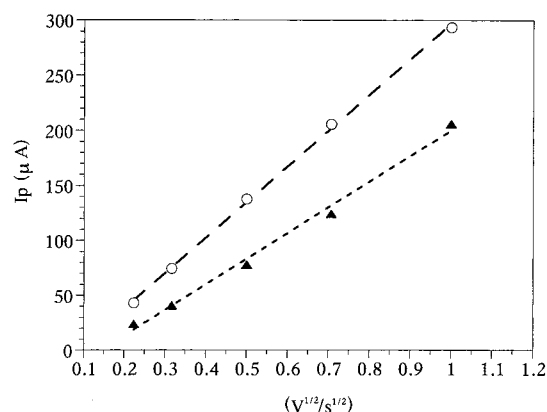


Figure 4. Dependence of the current of the anodic (▲) and cathodic (○) peaks associated with the PB/EVERITT's salt system on the square root of the scan rate for a DODA/PB LB film with 3 layers of PB.

space.³⁷ Similar results have been obtained with LB films with 2, 4, 6, and 8 layers of PB.

Impedance Spectroscopy. In the case of a film-modified electrode where the electroactive species is assumed to be fixed at the surface of the electrode, the diffusion impedance can be expressed as^{38–40}

$$Z_D = Z_0 \frac{\coth(\sqrt{j\omega\tau})}{\sqrt{j\omega\tau}} \quad (1)$$

with

$$\tau = \frac{l^2}{D} \quad (2)$$

where ω is the circular frequency, l is the diffusion length, and D is the apparent diffusion coefficient.

The impedance Z_D is represented in the complex plane by a linear branch at 45° at intermediate frequencies (corresponding

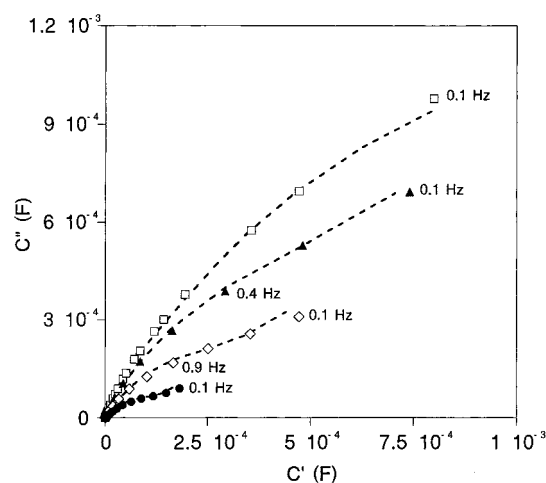


Figure 5. Complex plane plots of capacitance of DODA/PB LB films with (●) 1, (◇) 3, (▲) 6, and (□) 11 layers of PB in 0.5 M KCl at 0.2 V/SCE. Simulated curves (discontinuous lines) are obtained from the equivalent circuit shown in Figure 7.

to a semi-infinite diffusion regime) and a vertical branch at low frequencies.^{38,41} Such a behavior is typically obtained during the impedance study of polymer-film-modified electrodes.^{42,43} However, the vertical branch at low frequencies can only be observed if $\omega \ll D/L^2$.⁴⁴ This condition is difficult to satisfy in the case of very low values of the diffusion coefficient. In this situation, the impedance can be fitted by a simple semi-infinite Warburg term,⁴⁵ which is expressed⁴⁶

$$Z_D = \sigma \sqrt{\frac{2}{j\omega}} \quad (3)$$

where σ can be related to the diffusion coefficient by means of

$$\sigma = \frac{2\sqrt{2}RT}{n^2 F^2 A \sqrt{DC^0}} \quad (4)$$

where T is the temperature, R is the perfect gas constant, n is the number of electrons involved in the faradic process, F is the faraday constant, A is the electrode area, and C^0 is the volumic concentration in the electroactive species.

Moreover, in most of the real systems, the interface between the electroactive film and the electrode is not a perfectly smooth plane but has some roughness and/or porosity. Thus, an improved fit to experimental data is obtained when the ideal double-layer capacity is replaced by a constant phase element (CPE).^{40,47} The impedance of this element is given by an empirical formula:

$$Z_{CPE} = \frac{1}{K(j\omega)^m} \quad (5)$$

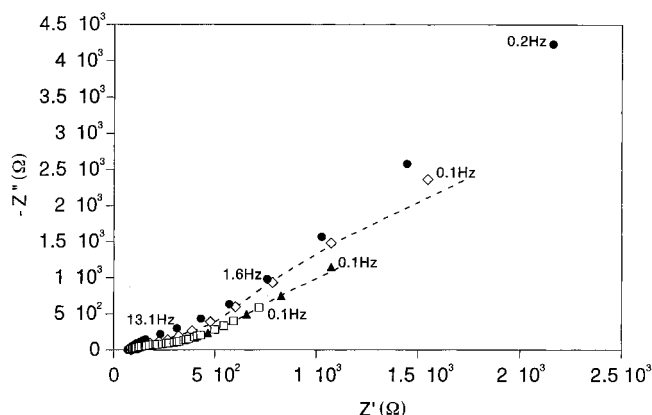
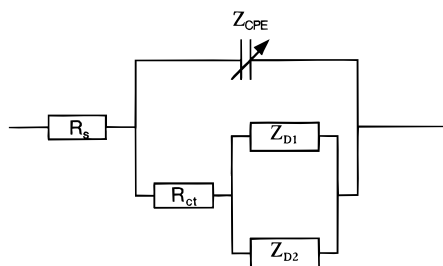
where K and m are two constants ($-1 \leq m \leq 1$). When $m = -1$, 0 , 1 , the CPE element transforms into a capacitance ($K = C$), a resistance ($K = 1/R$), and an inductance ($K = 1/L$), respectively.

Complex plane plots of capacitance and impedance of DODA/PB LB films with 1, 3, 6, and 11 layers of PB are shown in Figures 5 and 6, respectively. Capacitance is obtained from the impedance data by

$$C = \frac{1}{Z\omega j} \quad (6)$$

TABLE 3: Values of the Parameters of the Equivalent Circuit Shown in Figure 7 Obtained from the Fitting of the Experimental Impedance Data (Area of the Electrode $\approx 1.35 \text{ cm}^2$)

no. of PB layers	l (nm)	R_s (Ω)	R_{ct} ($\Omega \cdot \text{cm}^{-2}$)	Z_0 ($\Omega \cdot \text{cm}^{-2}$)	τ (s)	D_1 ($\text{cm}^2 \cdot \text{s}^{-1}$)	σ ($\Omega \cdot \text{s}^{-1/2}$)	D_2 ($\text{cm}^2 \cdot \text{s}^{-1}$)
1	2.5	69	51	4400	0.3	2.1×10^{-13}	6671	5.0×10^{-16}
3	11.3	83	86	2530	0.4	3.1×10^{-12}	2117	3.5×10^{-14}
6	24.5	95	152	3410	0.8	7.5×10^{-12}	1015	1.5×10^{-13}
11	46.5	82	140	3210	2.2	9.8×10^{-12}	810	1.4×10^{-13}

**Figure 6.** Complex impedance plane plots of DODA/PB LB films with (●) 1, (◇) 3, (▲) 6, and (□) 11 layers of PB in 0.5 M KCl at 0.2 V/SCE. Simulated curves (discontinuous lines) are obtained from the equivalent circuit shown in Figure 7 (for more clarity, only the simulated curves for 3 and 6 PB layers are given).**Figure 7.** Equivalent circuit used to simulate the impedance spectra of the DODA/PB LB films.

where C is the complex capacitance, Z is the complex impedance, ω is the angular frequency, and $j = (-1)^{1/2}$. The complex plane plots of capacitance show that the response of the LB films increases with the number of PB layers. Such a behavior has already been observed in the case of electrodeposited PB films on ITO electrodes.²⁹ This could be due to the charge transport processes through the lamellar systems. Besides, a straight line with an angle of slope between 45° and 90° can be observed at low frequencies in the Nyquist plots shown in Figure 6. It should indicate that two diffusive processes occur simultaneously during the oxidation/reduction of the DODA/PB LB films. In that way, the impedance spectra of the LB films could be represented by the Randles's modified equivalent circuit shown in Figure 7, which contains two transmission lines associated in parallel. Z_{D1} and Z_{D2} are a finite length transmission line and a semi-infinite Warburg impedance, respectively, to correspond to a fast and a slow charge transport processes across the lamellar materials. Similar equivalent circuits containing two transmission lines associated in parallel have been previously described in the literature to model impedance responses of electrodes coated with polymer^{42,44} or PB²⁹ films. To determine the parameters of the CPE, which reflects the double-layer capacitance at the ITO/first PB layer interface, the impedance spectrum of an uncovered ITO electrode has been fitted at 0.2 V/SCE using a R_s -CPE in series equivalent circuit. The following values have been obtained: $K = 1.14 \times 10^{-5} \text{ F} \cdot \text{s}^{1-m}$

and $m = 0.95$. These parameters were kept constant for all the other fits. R_s is the uncompensated ohmic drop. It was graphically determined as the high-frequency limit of the real part of impedance in Figure 6. R_{ct} is the charge transfer resistance due to an heterogeneous electron transfer between the ITO electrode and the LB film.

The resulting curves of the fitting procedure are shown in Figures 5 and 6 (discontinuous lines). It can be seen that the simulating curves reproduce quite well the experimental data. Table 3 collects the parameters obtained from the fit of the equivalent circuit to experimental data. The apparent diffusion coefficients D_1 and D_2 were calculated from eqs 2 and 4, respectively. It was assumed that the diffusion length was the total thickness of the LB film, which had been determined by X-ray diffraction studies.²⁴ The concentration of PB was calculated from the cyclic voltammetry measurements.

The low values of D_1 and D_2 observed in Table 3, which are 100 times smaller than those previously reported in the literature for electrodeposited PB films,²⁹ should reflect that the insulating lipid layers considerably hinder the diffusion of the charged species. The very low values of D_1 and D_2 in the case of the LB film with one PB layer should be due to the fact that the first transferred layer of PB is not organized according to the ideal structure of Langmuir–Blodgett films. Moreover, D_1 and D_2 both increase with the thickness of the lamellar materials. This indicates that the resistance of the films decreases when the number of deposited layers increases and thus should be related to the already mentioned presence of holes in the lipid layers. The physical meaning of the two diffusion coefficients could be interpreted in different ways. For example, D_1 could be a measure of electron transport and D_2 could be associated with the motion of the potassium ions through the LB films. Preliminary CV experiments in aqueous tetrabutylammonium bromide (Bu_4N^+) solutions have been carried out in order to better characterize the influence of the counterions on the electrochemical behavior of the DODA/PB LB films. Indeed, it is well-known that the size of the Bu_4N^+ ion is about 10 times larger than the K^+ ion's one. Thus, one should expect a modification of the CV curves of the hybrid LB films by changing the nature of the supporting electrolyte in such a way. In effect, a decrease of the intensity of the characteristic CV peaks of PB has been clearly observed, reflecting a poor penetration of the Bu_4N^+ ions in the lamellar systems. Impedance measurements are currently underway to determine whether changing the nature of the supporting electrolyte involves such a clear modification of the values of the diffusion coefficients D_1 and D_2 .

Conclusions

The voltammetric and impedance behaviors of new hybrid LB films containing PB have been studied in aqueous KCl solutions. In particular, it has been shown that the electrochemical coverage obtained by integration of the area of the CV peaks corresponds to one single layer of $\text{Fe}^{\text{II}}\text{--Fe}^{\text{III}}$, which is in agreement with the known structure of these hybrid materials. A straight line with an angle of slope between 45° and 90° has

also been observed at low frequencies in the Nyquist plots of the DODA/PB LB films, reflecting that two diffusive processes should occur simultaneously during their oxidation/reduction. An equivalent circuit with two transmission lines in parallel has been used to model such an impedance response. In conclusion, cyclic voltammetry and impedance spectroscopy are powerful tools to study the charge transport processes in complex materials such as DODA/PB LB films.

References and Notes

- (1) Neff, V. D. *J. Electrochem. Soc.* **1978**, *125*, 886.
- (2) Ellis, D.; Eckhoff, M.; Neff, V. D. *J. Phys. Chem.* **1981**, *85*, 1225.
- (3) Itaya, K.; Ataka, T.; Toshima, S. *J. Am. Chem. Soc.* **1982**, *104*, 4767.
- (4) Itaya, K.; Akahoshi, H.; Toshima, S. *J. Electrochem. Soc.* **1982**, *129*, 1498.
- (5) Itaya, K.; Uchida, I.; Neff, V. D. *Acc. Chem. Res.* **1986**, *19*, 162.
- (6) Itaya, K.; Uchida, I. *Inorg. Chem.* **1986**, *25*, 389.
- (7) Feldman, B. J.; Murray, R. W. *Anal. Chem.* **1986**, *58*, 2844.
- (8) Feldman, B. J.; Murray, R. W. *Inorg. Chem.* **1987**, *26*, 1702.
- (9) Dostal, A.; Meyer, B.; Scholz, F.; Schröder, U.; Bond, A. M.; Marken, F.; Shaw, S. J. *J. Phys. Chem.* **1995**, *99*, 2096.
- (10) Upadhyay, D. N.; Kolb, D. M. *J. Electroanal. Chem.* **1993**, *358*, 317.
- (11) Kulesza, P. J.; Zamponi, S.; Malik, M. A.; Miecznikowski, K.; Berrettoni, M.; Marassi, R. *J. Solid State Electrochem.* **1997**, *1*, 88.
- (12) Garcia-Jareno, J. J.; Navarro-Laboulais, J.; Vicente, F. *Electrochim. Acta* **1997**, *42*, 1473.
- (13) Garcia-Jareno, J. J.; Sanmatias, A.; Navarro-Laboulais, J.; Vicente, F. *Electrochim. Acta* **1998**, *44*, 395.
- (14) Roig, A.; Navarro, J.; Tamarit, R.; Vicente, F. *J. Electroanal. Chem.* **1993**, *360*, 55.
- (15) Garcia-Jareno, J. J.; Navarro-Laboulais, J.; Vicente, F. *Electrochim. Acta* **1996**, *41*, 2675.
- (16) Roig, A.; Navarro, J.; Garcia, J. J.; Vicente, F. *Electrochim. Acta* **1994**, *39*, 437.
- (17) Carpenter, M. K.; Conell, R. S. *J. Electrochem. Soc.* **1990**, *137*, 2464.
- (18) Duek E. A. R.; De Paoli, M. A.; Mastragostino, M. *Adv. Mater.* **1992**, *4*, 287.
- (19) Monk, P. M. S.; Mortimer, R. J.; Rosseinsky, D. R. *Electrochromism: Fundamentals and Applications*; VCH: Weinheim, 1995; Chapter 6.
- (20) Itaya, K.; Uchida, I.; Toshima, S. *J. Phys. Chem.* **1983**, *87*, 105.
- (21) Kaneko, M. *J. Macromol. Sci., Chem.* **1987**, *A24*, 357.
- (22) Kaneko, M.; Okada, T. *J. Electroanal. Chem.* **1988**, *255*, 45.
- (23) Neff, V. D. *J. Electrochem. Soc.* **1985**, *132*, 1382.
- (24) Mingotaud, C.; Lafuente, C.; Amiel, J.; Delhaes, P. *Langmuir* **1999**, *15*, 289.
- (25) Ravaine, S.; Lafuente, C.; Mingotaud, C. *Langmuir* **1998**, *14*, 6347.
- (26) Alberty, W. J.; Elliott, C. M.; Mount, A. R. *J. Electroanal. Chem.* **1990**, *288*, 15.
- (27) Alberty, W. J.; Mount, A. R. *J. Chem. Soc., Faraday Trans.* **1994**, *90*, 115.
- (28) Pickup, P. G. *J. Chem. Soc., Faraday Trans.* **1990**, *86*, 3631.
- (29) Garcia-Jareno, J. J.; Navarro, J. J.; Roig, A. F.; Scholl, H.; Vicente, F. *Electrochim. Acta* **1995**, *40*, 1113.
- (30) Garcia-Jareno, J. J.; Sanmatias, A.; Navarro-Laboulais, J.; Benito, D.; Vicente, F. *Electrochim. Acta* **1998**, *43*, 235.
- (31) Garcia-Jareno, J. J.; Navarro-Laboulais, J.; Vicente, F. *Electrochim. Acta* **1996**, *41*, 835.
- (32) Clemente-Leon, M.; Agricola, B.; Mingotaud, C.; Gomez-Garcia, C. J.; Coronado, E.; Delhaes, P. *Langmuir* **1997**, *13*, 2340.
- (33) Macdonald, J. R. LEVM program; University of North Carolina: Chapel Hill, NC, 1998.
- (34) Lüdi, A.; Güdel, H. U. *Structure and Bonding*; Dunitz, J. D., Ed.; Springer-Verlag: Berlin, 1973; Vol. 14, pp 1–21.
- (35) Herren, F.; Fischer, P.; Lüdi, A.; Hälg, W. *Inorg. Chem.* **1980**, *19*, 956.
- (36) Aoki, K.; Tokuda, K.; Matsuda, H. *J. Electroanal. Chem.* **1983**, *146*, 417.
- (37) Aoki, K.; Tokuda, K.; Matsuda, H. *J. Electroanal. Chem.* **1984**, *160*, 33.
- (38) Gabrielli, C.; Takenouti, H.; Haas, O.; Tsukada, A. *J. Electroanal. Chem.* **1991**, *302*, 59.
- (39) Ho, C.; Raistrick, I. D.; Huggins, R. A. *J. Electrochem. Soc.* **1980**, *127*, 343.
- (40) Bisquert, J.; Garcia-Belmonte, G.; Bueno, P.; Longo, E.; Bulhoes, L. O. S. *J. Electroanal. Chem.* **1998**, *452*, 229.
- (41) Mathias, M. F.; Haas, O. *J. Phys. Chem.* **1992**, *96*, 3174.
- (42) Amemiya, T.; Hashimoto, K.; Fujishima, A. *J. Phys. Chem.* **1993**, *97*, 9736.
- (43) Ren, X.; Pickup, P. G. *J. Electroanal. Chem.* **1997**, *420*, 251.
- (44) Rubinstein, I.; Rishpon, J.; Gottesfeld, S. *J. Electrochem. Soc.* **1986**, *133*, 729.
- (45) Franceschetti, D. R.; Macdonald, J. R. *J. Electroanal. Chem.* **1979**, *101*, 307.
- (46) Bard, A. J.; Faulkner, L. R. *Electrochemical Methods, Fundamentals and Applications*; Masson: Paris, 1983; pp 366.
- (47) Lindholm-Sethson, B. *Langmuir* **1996**, *12*, 3305.